Journal of Materials Chemistry C

Accepted Manuscript

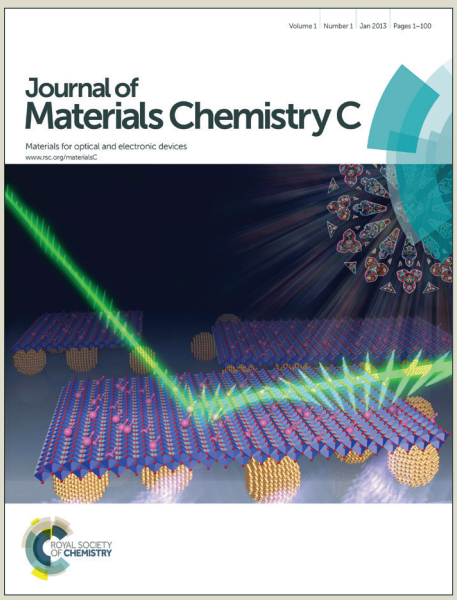

This is an *Accepted Manuscript*, which has been through the Royal Society of Chemistry peer review process and has been accepted for publication.

Accepted Manuscripts are published online shortly after acceptance, before technical editing, formatting and proof reading. Using this free service, authors can make their results available to the community, in citable form, before we publish the edited article. We will replace this *Accepted Manuscript* with the edited and formatted *Advance Article* as soon as it is available.

You can find more information about *Accepted Manuscripts* in the Information for Authors.

Please note that technical editing may introduce minor changes to the text and/or graphics, which may alter content. The journal's standard Terms & Conditions and the Ethical guidelines still apply. In no event shall the Royal Society of Chemistry be held responsible for any errors or omissions in this *Accepted Manuscript* or any consequences arising from the use of any information it contains.

ROYAL SOCIETY OF CHEMISTRY

www.rsc.org/materialsC

Journal of Materials Chemistry C

Cite this: DOI: 10.1039/c0xx00000x

PAPER

www.rsc.org/xxxxxx

Highly Efficient Single-layer Organic Light-emitting Devices Based on a Bipolar Pyrazine/Carbazole Hybrid Host Material

Yuan Liu, Lin-Song Cui, Mei-Feng Xu, Xiao-Bo Shi, Dong-Ying Zhou, Zhao-Kui Wang,* Zuo-Quan Jiang,* and Liang-Sheng Liao*

Received (in XXX, XXX) Xth XXXXXXXXX 20XX, Accepted Xth XXXXXXXXX 20XX
DOI: 10.1039/b000000x

Organic light-emitting diodes (OLEDs) have attracted tremendous interest and have already become the prevalent technology in MP3 players, smartphones and cameras. In response to the call for large-scale application of OLEDs, the complicated and costly process for preparing a device is a major challenge should be conquered. Herein, a novel bipolar host material 26PyzCz which contains the pyrazine/carbazole hybrid has been designed and synthesized. 26PyzCz-based single-layer (SL) fluorescent (F)/phosphorescent (P) OLEDs with various colors have been successfully fabricated. Green and orange SL phosphorescent OLEDs (PHOLEDs) have exhibited efficiencies as high as 63.3 and 62.1 cd A^{-1} at 1000 cd m^{-2}, and 55.7 and 53.8 cd A^{-1} at 10000 cd m^{-2}, respectively. Meanwhile, a SL warm white OLED based on fluorescent blue and phosphorescent orange has demonstrated excellent performance with a maximum current efficiency of 27.5 cd A^{-1} and a maximum power efficiency of 21.6 lm W^{-1}. In addition, the charge carrier behavior have been evaluated by impedance spectroscopy, which revealed that the dopant trapping effect plays a critical role on charge balance and exciton generation in the SL PHOLEDs.

Introduction

Organic light-emitting diodes (OLEDs) have attracted both scientific and industrial interest in flat-panel displays and solid-state lighting applications due to their lightweight body, low power consumption, flexibility, and so on.[1-3] The efficiency and brightness of state-of-the-art OLEDs could be dramatically improved by using phosphorescent emitters, which contain transition metal complexes especially the second- and third-row transition metals, with a fact of effective harvesting of both singlet and triplet exactions simultaneously through efficient intersystem crossing.[4,5] A typical OLED sandwiches emission layers within functional layers (such as the hole injection layer, hole transport layer, hole blocking layer, electron transport layer, electron injection layer etc.) to achieve balanced charge fluxes. In addition, many methods and techniques including electrode modification,[6] doping of transport layers,[7] charge/exciton confinement,[8, 9] emissive layer with mixed hosts,[10] stepwise doping[11] and tandem structure with multiple emission units,[12] have been developed to improve the device efficiency. In short, in order to pursue high-efficiency OLEDs, multilayer configuration is considered indispensable and has been widely used in most works. However, the use of these complicated device structures in OLEDs will inevitably increase the complexity of the production cycle and the fabrication cost, which introduces new obstacles on the way to OLEDs commercialization. On the other hand, the presence of heterojunction interfaces in the multilayer structure is unfavourable for the device stability owing to accumulation of charges and generation of higher electricfield at interfaces.[13,14] Therefore, there is strong incentive to develop simplified OLEDs. An "ideal simplified" structure consists of only one layer in a device due to least types of material are required and easy to be industrialized application. This layer has to bear the versatilities of the functional layers presented above. Therefore, the challenge becomes how to synthesize and incorporate a material that will act as the desired functional layer. This material must fulfill the requirements of an appropriate highest occupied molecular orbital (HOMO)/lowest unoccupied molecular orbital (LUMO), have a high triplet energy level suitable for dopants and high mobility for both electrons and holes. In theory, if we can get a host material with appropriate energy levels for hole/electron injection and transport, we could dope it with different guest emitters to achieve SL OLEDs.

Recently, SL OLEDs fabricated using some bipolar host materials, which possess both (more or less) hole and electron

Jiangsu Key Laboratory for Carbon-Based Functional Materials & Devices, Institute of Functional Nano & Soft Materials (FUNSOM); Collaborative Innovation Center of Suzhou Nano Science and Technology, Soochow University, Suzhou, Jiangsu 215123, China.
Email: zkwang@suda.edu.cn; zqjiang@suda.edu.cn; lsliao@suda.edu.cn.
Fax: +86-65882846. Tel: +86-512-65880945

† Electronic Supplementary Information (ESI) available. See DOI: 10.1039/b000000x/

Journal of Materials Chemistry C Accepted Manuscript

transport properties simultaneously, have been reported by several groups. Lin *et al*. developed a series of efficient SL OLEDs emitting blue light (2.5 cd A^{-1}, 2.5% of external quantum efficiency (EQE)),[15] green light (7.7 cd A^{-1}, 3.1% of EQE),[16] and orange light (5.21 cd A^{-1}, 1.43% of EQE).[17] To improve the device efficiency, Ma *et al*. reported a new carbazole/oxadiazole hybrid molecule as a bipolar host for SL green PHOLEDs with a maximum current efficiency up to 45.6 cd A^{-1}.[18] Lu *et al*. demonstrated a *N*-heterocyclic carbazole-based host (CBP-like) material for SL green PHOLEDs with a current efficiency up to 73.3 cd A^{-1} at 100 cd m^{-2}.[19] However, the development of SL OLEDs is severely limited by the absence of efficient bipolar host materials with excellent charge transport properties. Particularly, there are very few reports of the SL white OLEDs to this day.[20] Moreover, the operational mechanism including the charge carrier behavior in SL OLEDs, which is beneficial for the rational design and control of bipolar host materials, has rarely been studied directly while the device is in operation.

In this paper, we demonstrate a new carbazole/pyrazine hybrid bipolar host material, named as 2,6-bis(9-phenyl-9*H*-carbazol-3-yl) pyrazine (26PyzCz), for fabricating fluorescent (F)/phosphorescent (P) SL OLEDs with various colors. Green and orange SL PHOLEDs exhibit efficiencies as high as 63.3 and 62.1 cd A^{-1} at 1000 cd m^{-2}, and 55.7 and 53.8 cd A^{-1} at 10000 cd m^{-2}, respectively. Meanwhile, a SL warm white OLED based on fluorescent blue and phosphorescent orange demonstrates an excellent performance with a maximum current efficiency of 27.5 cd A^{-1} and a maximum power efficiency of 21.6 lm W^{-1}. Furthermore, the electrical transport properties such as the charge carrier behavior in the SL PHOLEDs are systematically investigated by using the impedance spectroscopy technique while the device is in operation. A circuit model is proposed to simulate the device performance based on the assumption that the dopant trapping effect plays a critical role during the exciton generation in the SL PHOLEDs.

Results and Discussion

Material Design and Physical Characteristics

Carbazole-based molecules have drawn tremendous attention as host materials in OLEDs due to their high triplet energy and excellent hole-transporting abilities.[21,22] In this molecular design, 2,6-bis(9-phenyl-9H-carbazol-3-yl) pyrazine (26PyzCz) was synthetized by introducing a strong electron-withdrawing subunit pyrazine as a spacer to connect two carbazole groups with the goal of balanced carrier transport. From the viewpoint of molecular topology, 26PyzCz was designed by directly connecting the pyrazine to the carbazole ring in the C3 position instead of connecting it to the *N*-phenyl ring based on a previous study that the former configuration will facilitate higher carrier transport.[22] The new material was synthesized via the classic Suzuki-Miyaura cross coupling reaction. Detailed synthetic procedures are described in the experimental section. The thermal characteristics were investigated by differential scanning calorimetry (DSC) and thermogravimetric analysis (TGA). T_g is clearly observed to be 127 ℃ with reversible cycles during heating and cooling. The decomposition temperature (T_d) with 5% loss is estimated to be 410 ℃ (Fig. S1). This suggests that a

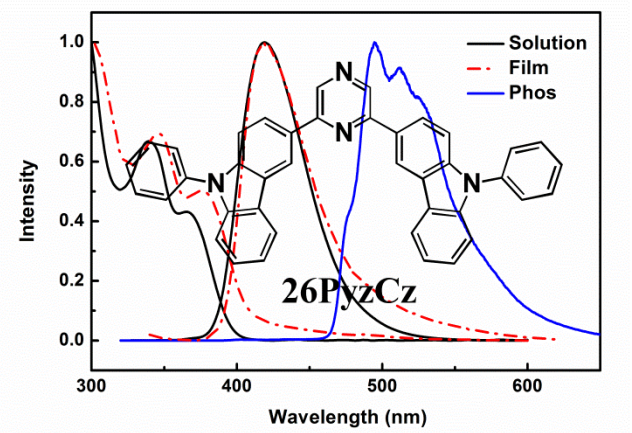

Fig. 1 UV-Vis absorption and PL spectra of 26PyzCz in dichloromethane solution as well as neat film and the phosphorescence spectra measured in frozen 2-methyltetrahydrofuran matrix at 77 K. The inset is the molecule structure of 26PyzCz.

morphologically stable and uniform amorphous film could be formed by vacuum deposition for OLEDs fabrication. Absorption, photoluminescence (PL), and low-temperature PL emission spectra of the 26PyzCz are shown in Fig. 1. The optical bandgap is 3.03 eV, calculated from the edge of the absorption spectrum of solid film. PL emission of 26PyzCz is observed at 418 nm, which is consistent with the film-based device (419 nm). This means that no significant intermolecular interactions occur in the ground state. The triplet energy of 26PyzCz is 2.51 eV, obtained from the first phosphorescent emission peak (λ= 494 nm) of the low-temperature PL spectrum measured at 77 K. Such high triplet energy is sufficient for 26PyzCz using as a host material for green/orange/red phosphors. All related physical parameters are summarized in Table S1.

The HOMO level of 26PyzCz measured by ultraviolet photoelectron spectroscopy (UPS) is 5.83 eV (Fig. S2) and the LUMO level is estimated to be 2.80 eV from the HOMO level and optical bandgap. The cyclic voltammetry (CV) result of 26PyzCz is shown in Fig. S3. Such LUMO and HOMO levels are suitable for efficient electron and hole injections, respectively. To understand the electronic structure of 26PyzCz at the molecular level, density function theory (DFT) calculations were performed at a B3LYP/6-31G (d) level for the geometry optimization (Fig. S4). The HOMO of 26PyzCz is situated on the entire molecule backbone because the nitrogen atom of carbazole can participate in the HOMO conjugation. On the other hand, the LUMO distribution is delocalized from the pyrazine center to the neighboring phenyl rings of the carbazole units. This suggests that the 26PyzCz, with the incorporation of a pyrazine group at the C3 position of carbazole, might possess improved electron-injection and transport properties compared to the unipolar carbazole derivatives.

To evaluate the carrier injection and transport properties of 26PyzCz, hole-only devices with a structure of ITO/MoO_3 (10 nm)/26PyzCz (or CBP) (100 nm)/MoO_3 (10 nm)/Al (120 nm) and electron-only devices with a structure of ITO/TmPyPB (10 nm)/ 26PyzCz (or CBP) (100 nm)/Liq (2 nm)/Al (120 nm) were fabricated. Molybdenum trioxide (MoO_3) and 1,3,5-tri[(3-pyridyl)- phen-3-yl]benzene (TmPyPB) were utilized to block electron and hole injection from the cathode and anode,

Journal of Materials Chemistry C Accepted Manuscript

This journal is © The Royal Society of Chemistry [year]

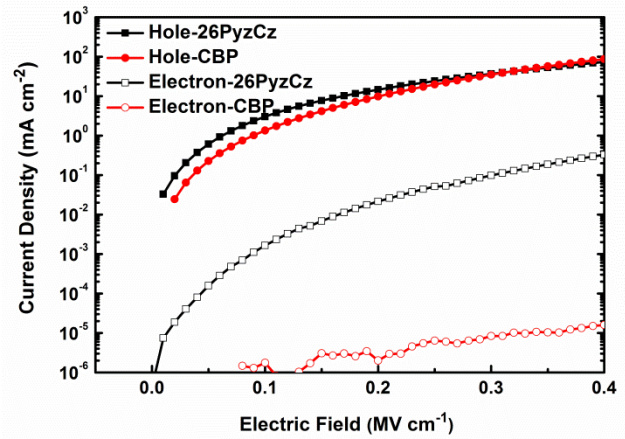

Fig. 2 The current density–voltage (*J*–*V*) curves for hole-only and electron-only devices.

respectively. Fig. 2 shows the current density versus voltage characteristics in the hole-only and the electron-only devices.

Obviously, the electron current density in 26PyzCz-based device is higher than that in CBP-based device, suggesting that 26PyzCz has better electron injection and transport properties than CBP. Meanwhile, the difference in current density between the hole-only and electron-only devices based on 26PyzCz is much smaller than that based on CBP at the same voltage. This means that 26PyzCz is a potential bipolar material capable of transporting electrons and holes by incorporating the electron-drawing moiety pyrazine and the electron-donating unit carbazole.

OLED performance

Monochrome OLEDs

Utilizing the ambipolar property of 26PyzCz, blue, green and orange SL monochrome OLEDs were fabricated with the same device configuration of ITO/MoO_3 (5 nm)/**26PyzCz** (40 nm)/**26PyzCz**: dopants (30 nm)/**26PyzCz** (30 nm)/Liq (2 nm)/Al (120 nm). The doped 26PyzCz, acting as an emission layer (EML) was inserted between two undoped 26PyzCz layers which serve as a hole transport layer as well as an electron transport layer. In the EMLs, 26PyzCz was doped by 6% $Ir(ppy)_2(acac)$ and 6% PO-01 for phosphorescence green and orange emission, respectively, and 3% DSA-Ph for fluorescence blue emission to cater to the mass fervor of fluorescence-phosphorescence hybrid white OLEDs.[23,24] Fig. 3 displays the relative energy levels and

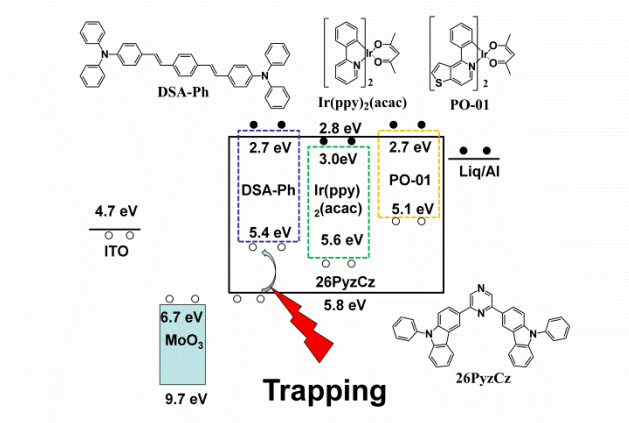

Fig. 3 Energy levels and molecular structures of the materials for the devices.

molecular structures of the materials adopted in these devices. The devices exhibit typical emissions that originate from the dopants of DSA-Ph, $Ir(ppy)_2(acac)$ and PO-01, with peaks located at 476 nm, 524 nm and 564 nm, respectively (Fig. S5).

Fig. 4(a) illustrates the current density-voltage-luminance (*J*-*V*-*L*) characteristics of these devices. The operating voltage in the green-device (6.7 V) at 20 mA cm^{-2} is lower than that in both blue and orange devices (7.0 V), which is presumably attributed to the different trapping effect of the dopants. It has been reported that the doped emitters can capture the charge carriers directly and the trapping ability of holes (electrons) strongly depends on the gap between the HOMO (LUMO) levels of the emitter molecule and the matrix molecule.[25] The material mobility can be approximated as[26]

$$\mu \propto \exp\left(-\frac{E_0-\beta\sqrt{F}}{KT}\right) \quad (1)$$

where E_0 is the zero-field activation energy, β the Poole-Frenkel constant, F the external electric field strength, and KT is the thermal energy at temperature T. For doped materials, E_0 is mostly determined by the energy level difference between the host material and the dopant. In present devices, the dopants actually serve as the deep trapping states for holes while the shallow trapping states for electrons with respect to significantly different gaps of HOMO and LUMO levels between the host and the dopants (as seen in Fig. 3). Therefore, as the HOMO level of a dopant becomes shallower, a higher driving voltage is required. Also, the direct charge hopping between the emitter molecules, which strongly depends on the dopant concentration, should be considered.[27] Taking into account the two pathways for charge transport, it is understandable that the blue emitting device, which has deeper dopant HOMO level and a lower doping concentration, need the same driving voltage as that of the green emitting device.

The efficiency versus luminance curves are displayed in Fig. 4(b) and the detailed efficiency characteristics are summarized in Table 1. The DSA-Ph-based fluorescence blue device exhibits a maximum current efficiency of 12.0 cd A^{-1} and a maximum power efficiency of 9.3 lm W^{-1} with a voltage of 4.0 V and CIE of (0.17, 0.39) at 24 cd m^{-2}. The $Ir(ppy)_2(acac)$-based green and PO-01-based orange devices show attractive EL efficiencies (65.5 cd A^{-1}, 52.1 lm W^{-1} and 65.5 cd A^{-1}, 51.9 lm W^{-1}) at 131 cd m^{-2} which are among the best levels in reported SL OLEDs.[19] Furthermore, the efficiency roll-offs are impressively low. At the practical brightness of 1000 cd m^{-2} and even at the high brightness of 10000 cd m^{-2}, the current efficiency roll-offs are only 3% (63.3 cd A^{-1}) and 15% (55.7 cd A^{-1}) for green and 5% (62.1 cd A^{-1}) and 17% (53.8 cd A^{-1}) for orange, respectively.

White OLED

The excellent SL monochrome OLEDs inspired us to further investigate the performance of 26PyzCz for SL White OLEDs.[28] Thus, a fluorescent/phosphorescent (F-P) hybrid warm white OLED with the structure of ITO/MoO_3 (5 nm)/**26PyzCz** (40 nm)/**26PyzCz**: 3% DSAph (10 nm)/**26PyzCz** (5 nm)/**26PyzCz**: 6% PO-01 (15nm)/**26PyzCz** (30 nm)/Liq (2 nm)/Al (120 nm) was fabricated. The proposed device can be referred to as a single-layer (SL) structure since only one homogenous organic layer of 26PyzCz is contained in the device.[18] Fig. 5 shows the

Journal of Materials Chemistry C Accepted Manuscript

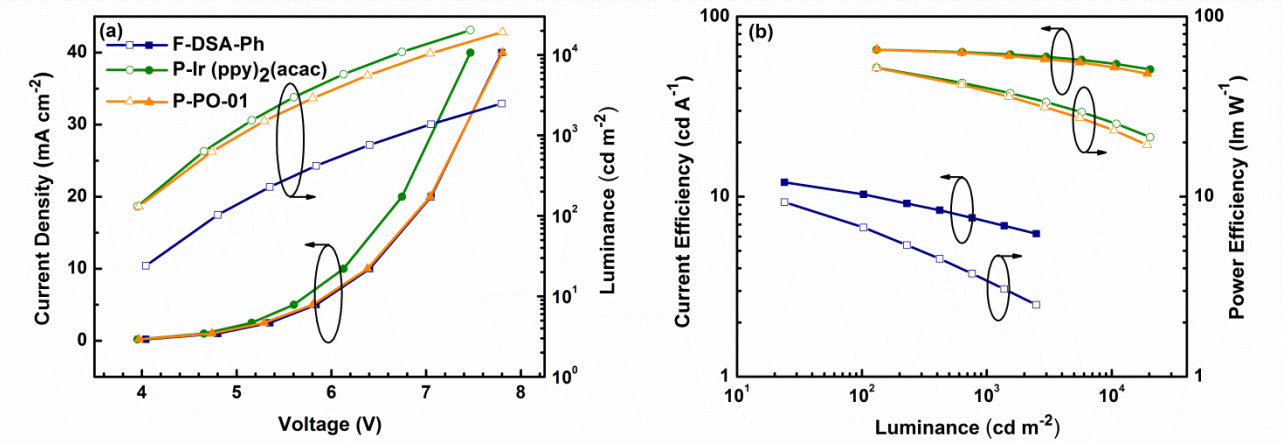

Fig. 4 (a) Current density-voltage-luminance (*J*–*V*–*L*) characteristics, (b) current efficiency and power efficiency versus luminance of monochrome OLEDs.

Table 1 Summary of OLEDs Performances.

Device (Host/dopants)	$\eta_{c.max}/\eta_{p.max}$ [cd A^{-1}/lm W^{-1}][a)]	$\eta_{c,500}/\eta_{P,500}$ [cd A^{-1}/lm W^{-1}][b)]	$\eta_{c,1000}/\eta_{P,1000}$ [cd A^{-1}/lm W^{-1}][c)]	CIE (x,y)[d)]
Blue (DSA-Ph)	12.0/9.3	8.3/4.6	7.5/3.8	0.17 0.39
Green ($Ir(ppy)_2(acac)$)	65.5/52.1	64.3/44.5	63.3/40.5	0.31 0.64
Organge (PO-01)	65.5/51.9	63.8/43.3	62.1/39.5	0.48 0.50
White (F-P)	27.5/21.6	25.1/15.5	23.9/13.6	0.41 0.46

[a)] Maximum current efficiency ($\eta_{c.max}$) and Maximum power efficiency ($\eta_{p.max}$); [b)] current efficiency (η_c) and power efficiency (η_p) at 500 cd m^{-2}; [c)] η_c and η_p at 1000 cd m^{-2}; [d)]Commission International de I'Eclairage coordinates measured at 5 mA cm^{-2}.

current efficiency and power efficiency characteristics of the white device and the inset is its corresponding electroluminescence spectrum. The device obtained maximum current efficiency of 27.5 cd A^{-1} and power efficiency of 21.6 lm W^{-1}, respectively. Noticeably, there exists no organic/organic heterojunctions in the device. This helps to eliminate the redundant interfaces near the exciton formation zones and avoids charge-carrier accumulation, generation of higher electricfield and exciton quenching at interfaces. Thus, the device lifetime is expected to be longer than conventional multilayer F-P hybrid white OLEDs.[13,29-32]

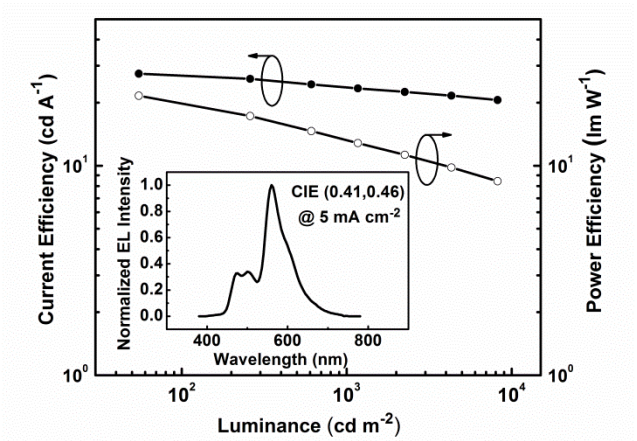

Fig. 5 Current efficiency and power efficiency versus luminance of white OLED. The inset is the EL spectrum at 5 mA cm^{-2}.

Operation Mechanism of Single Layer OLEDs

As mentioned above, the operational mechanism in SL OLEDs is presently not well understood. Herein, we investigate the charge carrier behaviour with an impedance spectrum from the SL orange PHOLEDs while the device is in operation.

Carrier behaviour

The impedance versus bias voltage (*Z*-*V*) and phase versus bias voltage (θ-*V*) characteristics measured at various frequencies in 26PyzCz: PO-01 based SL OLEDs are depicted in Fig. 6. From *Z*-*V* curves, an obvious transition in impedance corresponding to a characteristic transition voltage (V_c) was observed at various frequencies. This is ascribed to a decrease in the dielectric relaxation time due to the injection behaviour of charge carriers into the device. As seen in Fig. 2, the hole injection is easier than the electron injection. Hence, in the present case, V_c represents the beginning of electron injection[33] and shows a considerable frequency dependence due to the deterioration of electron-injection ability by the alternating current (AC) electric field. As

This journal is © The Royal Society of Chemistry [year]

Journal of Materials Chemistry C Accepted Manuscript

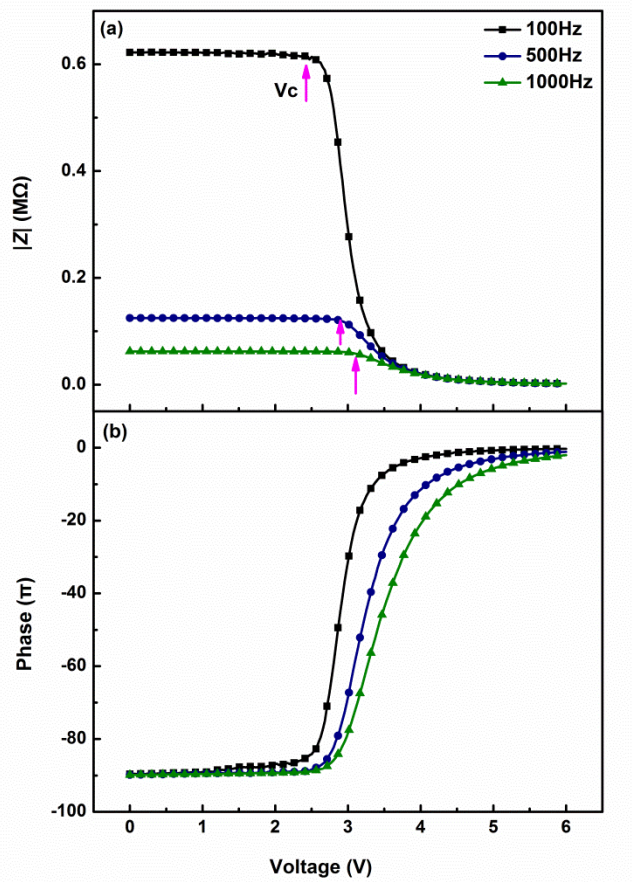

Fig. 6 (a) *Z-V*, (b) *θ-V* characteristics of the device measured at the frequencies of 100 Hz, 500 Hz and 1000 Hz, respectively.

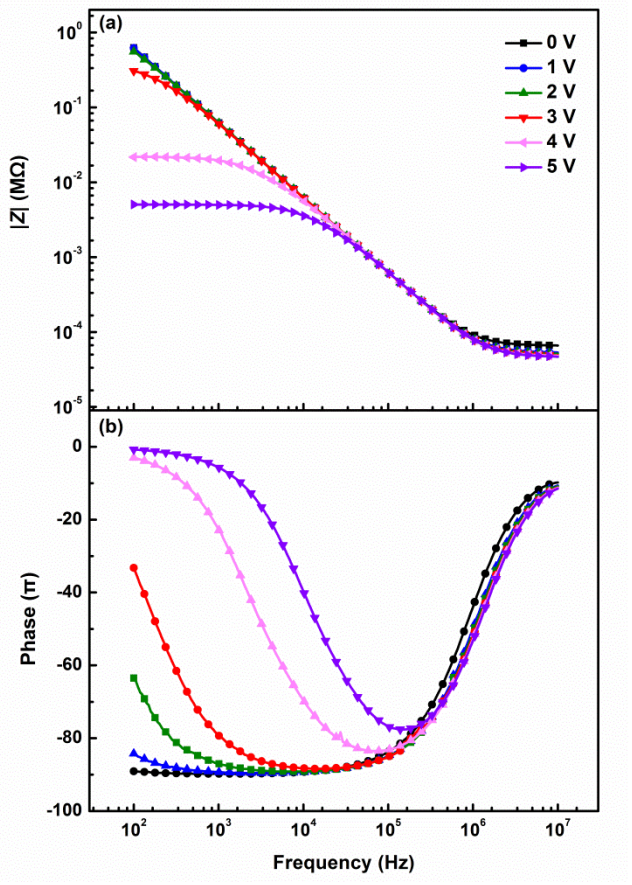

Fig. 7 (a) Modulus spectra, (b) phase spectra of the device under different applied voltage.

seen from the *θ-V* curves, the device exhibits purely capacitive response when the driving voltage is lower than V_c. With further increase of the applied voltage, a non-negligible drift current appears and the phase θ deviates from –π/2 to 0, This corresponds to conductive behaviour and an electron-hole recombination process. For example, in the case of 100 Hz, electrons can be effectively injected into the device and recombine with holes over 2.5 V, which is consistent with the analysis of current density-voltage (*I-V*) and capacitance-voltage (*C-V*) characteristics (Fig. S6). It is apparent that 26PyzCz containing an electron-withdrawing pyrazine group possesses a well-matched LUMO to the work function of the cathode and improved electron-injection and transport properties.

Trapping mechanism

In general, dopant in a host: dopant system tends to act as a charge trapping center or an additional transporting channel. Both of these significantly influence the charge transport ability.[34] From the energy levels of 26PyzCz and dopants revealed in Fig. 3 and the *J-V-L* characteristics of monochrome OLEDs, the dopants are inclined to act as the hole trapping states in our devices.

As depicted in Fig. 7(a), the modulus curves show two obvious plateaus in the low- and high-frequency regions. For the capacitance attribution, the modulus changes with 1/(ωP) in the medium frequency range, which agrees with a common equivalent circuit containing a single RC parallel circuit plus a series resistance.[35] However, an interesting feature appears in the phase spectrum as displayed in Fig. 7(b). At voltages higher than 4V, only one peak emerges. While at low bias (< 4V), an additional peak around 1 KHz is observed. This means that there are at least two RC times in the device. We ascribed it to the trapping states that originated from PO-01 dopants.

Based on the analysis from impedance spectra measurement, an equivalent circuit model is proposed and shown in Fig. 8(a). R_s represents the series resistance due to the effect of contacts, R_p and C_p are the resistance and geometric capacitance of the intrinsic layer, and C_t and R_t correspond to the contributions from trapping states. For simplicity, the dopant trapping states are described with one discrete intra-gap state. By carefully adjusting the circuit parameters (R_s, R_p, S_p, R_p, C_p), the simulated spectra using the equivalent circuit agreed well with the measured data as shown in Fig. 8(b). The detailed values of element parameters are summarized in Table 2. The capacitance values (C_p and C_t) roughly stay constant, while R_p and R_t decrease sharply with the voltage increase because of the injection of carriers. By combining these data and the aforementioned performance of the charge only devices and electroluminescence spectrum, it can be concluded that: i) 26PyzCz possess improved electron-injection and transport properties with the incorporation of an electron-withdrawing pyrazine group compared to those unipolar carbazole derivatives; ii) actually the injection and transport performances of holes are better than the performances of electrons; iii) the dopants act as deep trapping states for the holes while shallow trapping states for electrons, and the charge balance is greatly enhanced by carrier trapping effect; iv) because

Journal of Materials Chemistry C Accepted Manuscript

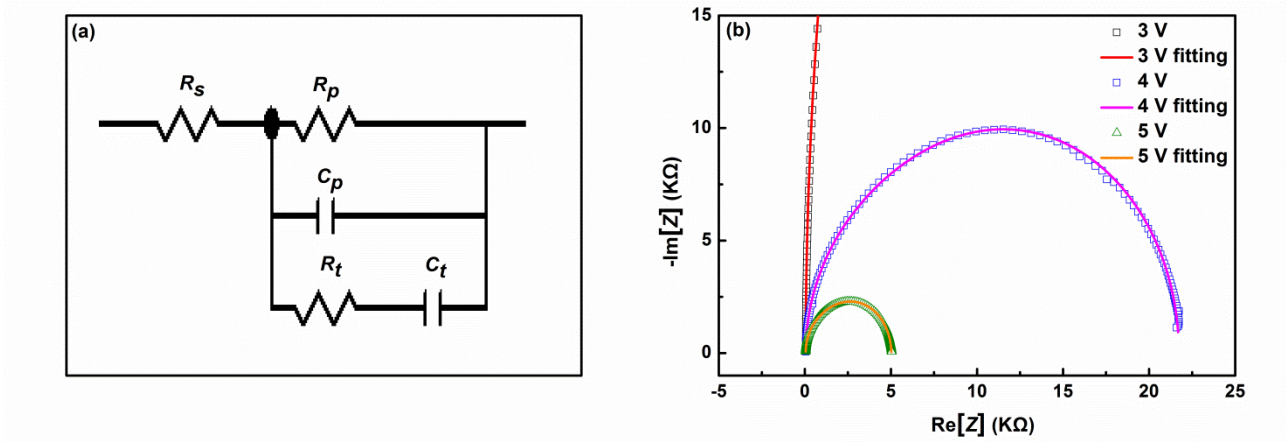

Fig. 8 (a) The equivalent circuit; (b) measured Cole–Cole plots and optimized fittings of the device for different bias voltages.

Table 2 Summary of the parameters obtained from fitting the measured data by the equivalent circuit in Fig. 8(a).

Bias (V)	R_s [Ω]	R_p [KΩ]	C_p [nF]	R_t [KΩ]	C_t [nF]
3 V	51.39	377.44	2.55	1952.22	0.40
4 V	48.52	21.68	2.54	57.03	0.63
5 V	46.46	4.98	2.52	18.22	0.52

of the trapping effect, the excitons are mainly generated on the dopants when the driving voltage is lower than 4 V. Additionally, the process of exciton generation on the host and then subsequent harvest by the dopants also exist in a higher driving voltage; v) the excitons are well confined in the emission layers with respect to the electroluminescence spectra of devices.

Taking into account the trapping effect, two phenomena are worthwhile to note： i) As holes get trapped in the dopant molecules to reduce electron–electron repulsion, the LUMO levels of dopants shift to lower and electron injection becomes easier.[9] This contributes to a low driving voltage. ii) Combined with the bipolar characteristic of 26PyzCz, the hole trapping effect of dopants results in a broad recombination zone,[18,36] which corresponds to the low roll-offs of the devices efficiencies.

Conclusions

In conclusion, we have synthesized and characterized a new bipolar material 26PyzCz by introducing a strong electron-withdrawing subunit pyrazine. The corresponding SL blue (F), green (P), orange (P) monochrome and F-P hybrid warm white OLEDs achieved the maximum power efficiencies of 9.3 lm W^{-1}, 52.1 lm W^{-1}, 51.9 cd A^{-1}, 21.6 lm W^{-1}, respectively. All SL OLEDs exhibit low efficiency roll-offs. Additionally, we carried out an investigation on the charge carrier behaviour and the trapping mechanism in the SL PHOLEDs based on impedance spectroscopy measurements. The experimental results demonstrate that the dopant trapping effect plays a critical role on charge balance and exciton generation in the SL OLEDs. This can provide helpful information for further work in the simpler and more practical SL OLEDs.

Experimental Section

Materials and General Instrumentation

[3-(9H-carbazol-9-yl)phenyl] boronic acid and 2,6-dibromopyrazine were purchased from Bepharm limited. Tetrakis (triphenylphosphine)-palladium (0) [$Pd(PPh_3)_4$] was obtained from Strem Chemicals. All other chemicals were obtained from commercial sources (Sinopharm, Aladdin, and TCI) and used as received without further purification. THF was purified by the PURE SOLV (Innovative Technology) purification system. Chromatographic separations were carried out by using silica gel (200-300 nm).

^{1}H NMR and ^{13}C NMR spectra were recorded on a Varian Unity Inova 400 spectrometer at room temperature. Mass spectra were obtained on a Thermo ISQ mass spectrometer by using a direct exposure probe. UV-Vis absorption spectra were recorded on a Perkin Elmer Lambda 750 spectrophotometer. PL spectra and phosphorescent spectra were carried out on a Hitachi F-4600 fluorescence spectrophotometer. Differential scanning calorimetry (DSC) was performed on a TA DSC 2010 unit at a heating rate of 10 ^oC min^{-1} in a nitrogen atmosphere. The glass transition temperatures (T_g) were determined from the second heating scan. Thermo gravimetric analysis (TGA) was performed on a TA SDT 2960 instrument at a heating rate of 10 ^oC min^{-1} in a nitrogen atmosphere. Temperature at 5% weight loss was used as the decomposition temperature (T_d). Cyclic voltammetry (CV) was carried out on a CHI600 voltammetric analyzer at room temperature with a conventional three-electrode configuration consisting of a platinum disk working electrode, a platinum wire auxiliary electrode, and an Ag wire pseudo-reference electrode with ferrocenium–ferrocene (Fc^+/Fc) as the internal standard. Nitrogen-purged dichloromethane was used as the solvent for the oxidation scan and DMF for the reduction scan with tetrabutylammonium hexafluorophosphate (TBAPF6) (0.1 M) as the supporting electrolyte. The cyclic voltammograms were obtained at a scan rate of 100 mV s^{-1}.

2,6-bis(9-phenyl-9H-carbazol-3-yl)pyrazine (26PyzCz)

In a 100 mL flame-dried two-necked flask, [3-(9H-carbazol-9-

This journal is © The Royal Society of Chemistry [year]

Journal of Materials Chemistry C Accepted Manuscript

yl)phenyl] boronic acid (2.65 g, 9.25 mmol), 2,6-dibromopyrazine (1.0 g, 4.20 mmol), and $Pd(PPh_3)_4$ (0.53 g, 0.46 mmol) were added and subjected to three vacuum/nitrogen fill cycles. Nitrogen-degassed THF (40 mL) and aqueous 2 M K_2CO_3 solution (10 mL) were subsequently added. The reaction mixture was heated to 60 °C for 8 h in an argon atmosphere. After cooling to room temperature, the organic layer was separated and evaporated to remove the solvent. The residue was purified by column chromatography with 1:3 (v/v) dichloromethane/petroleum ether as the eluent and recrystallized from dichloromethane/petroleum to produce the final product as a yellow solid (2.17 g, 92%).^{1}H NMR (400 MHz, $CDCl_3$) δ (ppm): 9.06 (s, 2H) 8.99 (d, J = 16.0 Hz, 2H) 8.32-8.25 (m, 4H) 7.69-7.41 (m, 16H) 7.40-7.30 (m, 2H). ^{13}C NMR (100 MHz, CDCl3) δ (ppm): 152.4, 141.9, 141.5, 138.6, 137.3, 130.0, 128.7, 127.8, 126.4, 125.2, 124.0, 123.5, 120.6, 120.48, 119.3, 110.3, 110.1 MS (EI): m/z 562.46 [M^+]. Anal. calcd for $C_{36}H_{24}N_2$ (%): C 85.38, H 4.66, N 9.96; found: C 85.26, H 4.59, N 10.18.

Device Fabrication and Measurements

The OLED devices were fabricated on commercially available ITO-coated glass substrates, which were ultrasonically cleaned with a standard regiment of acetone, methanol, and deionized water for 5 min each, dried at 120 ℃ and treated by UV ozone for 5 min. All layers were deposited under a base pressure of 2×10^{-6} Torr. The deposition rates and doping concentration of the films were monitored in situ by the calibrated thickness monitors. The typical evaporation rate for MoO_3, organic layer and Liq were 0.4-0.8, 2-3 and 0.2-0.5 Å s^{-1}, respectively. Finally, the Al electrode was evaporated (5 Å s^{-1}) through a shadow mask without breaking the vacuum. The active area of each device was 3×3 mm^2. Electroluminescence (EL) and current-voltage (*I-V*) characteristics were measured by a constant current source (Keithley 2400s Source Meter) combined with a photometer (Photo Research PR 655 spectrophotometer). The impedance spectroscopy (*IS)* measurements were taken by Wayne Kerr 6550B precision impedance analyzer in a frequency range from 100 Hz to 10 MHz, with 30 mV perturbation oscillation signal.

Acknowledgements

We acknowledge financial support from the Natural Science Foundation of China (Nos. 61036009, 61177016, and 21161160446), and the Key University Science Research Project of Jiangsu Province (12KJB510028). This is also a project funded by the Priority Academic Program Development of Jiangsu Higher Education Institutions (PAPD) and by the Fund for Excellent Creative Research Teams of Jiangsu Higher Education Institutions.

Notes and references

1. K. T. Kamtekar, A. P. Monkman, M. R. Bryce, *Adv. Mater.*, 2010, **22**, 572.
2. L. Xiao, Z. Chen, B. Qu, J. Luo, S. Kong, Q. Gong, J. Kido, *Adv. Mater.*, 2011, **23**, 926.
3. H. Sasabe, J. Kido, *J. Mater. Chem. C*, 2013, **1**, 1699.
4. M. A. Baldo, D. F. O'Brien, Y. You, A. Shoustikov, S. Sibley, M. E. Thompson, S. R. Forrest, *Nature*, 1998, **395**, 151.
5. L. S. Hung, C. H. Chen, *Mater. Sci. Eng., R*, 2002, **39**, 143.
6. C. H. Gao, S. D. Cai, W. Gu, D. Y. Zhou, Z. K. Wang, L. S. Liao, *Acs Appl. Mater. Interfaces*, 2012, **4**, 5211.
7. K. Walzer, B. Maennig, M. Pfeiffer, K. Leo, *Chem. Rev.*, 2007, **107**, 1233.
8. B. D. Chin, C. Lee, *Adv. Mater.*, 2007, **19**, 2061.
9. C. H. Gao, D. Y. Zhou, W. Gu, X. B. Shi, Z. K. Wang, L. S. Liao, *Org. Electron.*, 2013, **14**, 1177.
10. J. H. Lee, C. I. Wu, S. W. Liu, C. A. Huang, Y. Chang, *Appl. Phys. Lett.*, 2005, **86**, 103506.
11. B. D. Chin, M. C. Suh, M. H. Kim, S. T. Lee, H. D. Kim, H. K. Chung, *Appl. Phys. Lett.*, 2005, **86**, 133505.
12. L. S. Liao, W. K. Slusarek, T. K. Hatwar, M. L. Ricks, D. L. Comfort, *Adv. Mater.*, 2008, **20**, 324.
13. H. Aziz, Z. D. Popovic, N.-X. Hu, A.-M. Hor, G. Xu, *Science*, 1999, **283**, 1900.
14. Z. K. Wang, Y. H. Lou, S. Naka, H. Okada, *Acs Appl. Mater. Interfaces*, 2011, **3**, 2496.
15. M. Y. Lai, C. H. Chen, W. S. Huang, J. T. Lin, T. H. Ke, L. Y. Chen, M. H. Tsai, C. C. Wu, *Angew. Chem. Int. Ed.*, 2008, **47**, 581.
16. T. H. Huang, J. T. Lin, L. Y. Chen, Y. T. Lin, C. C. Wu, *Adv. Mater.*, 2006, **18**, 602.
17. K. R. J. Thomas, J. T. Lin, M. Velusamy, Y. T. Tao, C. H. Chuen, *Adv. Funct. Mate*r., 2004, **14**, 83.
18. X. Qiao, Y. Tao, Q. Wang, D. Ma, C. Yang, L. Wang, J. Qin, F. Wang, *J. Appl. Phys.*, 2010, **108**, 034508.
19. Z. M. Hudson, Z. Wang, M. G. Helander, Z. H. Lu, S. Wang, *Adv. Mater.*, 2012, **24**, 2922.
20. Y. Yin, X. Piao, Y. Li, Y. Wang, J. Liu, K. Xu, W. Xie, *Appl. Phys. Lett.*, 2012, **101**, 063306.
21. M. H. Tsai, Y. H. Hong, C. H. Chang, H. C. Su, C. C. Wu, A. Matoliukstyte, J. Simokaitiene, S. Grigalevicius, J. V. Grazulevicius, C. P. Hsu, *Adv. Mater.*, 2007, **19**, 862.
22. L. S. Cui, S. C. Dong, Y. Liu, Q. Li, Z. Q. Jiang, L. S. Liao, *J. Mater. Chem. C*, 2013, **1**, 3967.
23. Y. Sun, N. C. Giebink, H. Kanno, B. Ma, M. E. Thompson, S. R. Forrest, *Nature*, 2006, **440**, 908.
24. G. Schwartz, S. Reineke, T. C. Rosenow, K. Walzer, K. Leo, *Adv. Funct. Mater.*, 2009, **19**, 1319.
25. N. Matsusue, S. Ikame, Y. Suzuki, H. Naito, *Appl. Phys. Lett.*, 2004, **85**, 4046.
26. T. Minari, T. Nemoto, S. Isoda, *J. Appl. Phys.*, 2006, **99**, 034506.
27. Y. Olivier, V. Lemaur, J. L. Bredas, J. Cornil, *J. Phys. Chem. A*, 2006, **110**, 6356.
28. S. Reineke, F. Lindner, G. Schwartz, N. Seidler, K. Walzer, B. Lussem, K. Leo, *Nature*, 2009, **459**, 234.
29. M. C. J. M. Vissenberg, M. Matters, *Phys. Rev. B*, 1998, **57**, 12964.
30. Z. K. Wang, H. Okada, S. Naka, *Jpn. J. Appl. Phys.*, 2010, **49**, 01AA02.
31. Z. K. Wang, Y. H. Lou, S. Naka, H. Okada, *Appl. Phys. Lett.*, 2010, **97**, 203302.
32. F. So, D. Kondakov, *Adv. Mater.*, 2010, **22**, 3762.
33. S. Berleb, W. Brütting, G. Paasch, *Org. Electron.*, 2000, **1**, 41.
34. F. Nüesch, D. Berner, E. Tutiš, M. Schaer, C. Ma, X. Wang, B. Zhang, L. Zuppiroli, *Adv. Funct. Mater.*, 2005, **15**, 323.

Journal of Materials Chemistry C Accepted Manuscript

35. L. Burtone, D. Ray, K. Leo, M. Riede, *J. Appl. Phys.*, 2012, **111**, 064503.
36. S. J. Su, E. Gonmori, H. Sasabe, J. Kido, *Adv. Mater.*, 2008, **20**, 4189.

Journal of Materials Chemistry C Accepted Manuscript

This journal is © The Royal Society of Chemistry [year]

Table of Contect

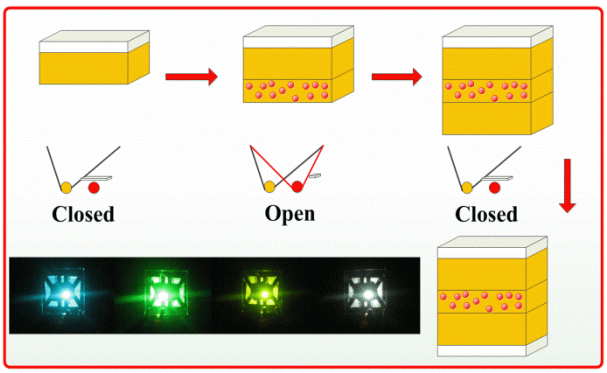

High efficiency blue (F), green (P), orange (P) and F-P hybrid warm white single-layer OLEDs fabricated through simple manufacturing process.

Journal of Materials Chemistry C Accepted Manuscript